[(thf)Li$_2${H$_2$CS(N^{t}Bu)$_2$}]$_2$: Synthesis, Polymorphism, and Experimental Charge Density to Elucidate the Bonding Properties of a Lithium Sulfur Ylide

Stephan Deuerlein, Dirk Leusser, Ulrike Flierler, Holger Ott, and Dietmar Stalke*

Institut für Anorganische Chemie, Universität Göttingen, Tammannstrasse 4, 37077 Göttingen, Germany

Received January 16, 2008

Sulfur ylides ($R_2S^+-{}^-CR_2$) are widely used in organic synthesis for stereoselective epoxidations, cyclopropane formations, and ring expansion reactions. Nevertheless, their electronic properties are still under debate, because their ylenic textbook formulation ($R_2S{=}CR_2$) contradicts the reactivity. In order to elucidate the electronic situation in a sulfur ylide, we present an experimental charge density study via multipole refinement and subsequent topological analysis based on high-resolution X-ray data of [(thf)Li$_2${H$_2$CS(N^{t}Bu)$_2$}]$_2$ (**1**). The title compound is of special interest, since additionally the formal hypervalency can be investigated along with the controversial interaction between a carbanion with a Li_3 triangle. As a prerequisite for these studies, the polymorphism and synthesis of **1** were investigated. The findings clearly support the ylidic, non-hypervalent description of the molecule. The ylidic carbanion was determined to be 6-fold coordinated with three single bonds to the sulfur atom and both hydrogen atoms and three closed-shell interactions to the lithium atoms of the Li_3 triangle.

Introduction

Sulfonium ylides and Corey's sulfoxonium ylides ($R_2(O)S^+-{}^-CR_2$) play an important role in organic syntheses. Scheme 1 displays the synthetic versatility of sulfur ylides. They are mainly used in CR_2-transfer reactions (e.g. in stereoselective epoxidations). In contrast to the two-step synthesis facilitating a Wittig reagent ($R_3P^+-{}^-CR_2$), sulfur ylides can be used as one-step epoxidating agents.[1] Additionally, stereospecific cyclopropanation[2] and aziridination[3] reactions are available for activated sulfur ylide complexes. The use of sulfur ylides ($(RN)_{2/3}S^+-{}^-CR_2$) allows transimidation reactions by choice of the experimental conditions (particularly the temperature).[4]

Nevertheless, the bonding properties of this important class of reagents are still under debate. The S−C as well as the S−N bond cleavages[5] clearly contradict the classical Lewis notation of S=C or S=N double bonds (hypervalent ylenic form, cf. Scheme 2a).[6] Thus, an ylidic resonance form seems much more feasible (cf. Scheme 2b−d).[7] This fuels the dispute to what extent sulfur ylides are dominated by *ylidic* or *ylenic* bonding. Experimental charge density studies clearly are the appropriate tool to decide on this question as similar issues with the sulfurtriimide S(N^{t}Bu)$_3$ could be explained by these means.[8] [(thf)Li$_2${H$_2$CS(N^{t}Bu)$_2$}]$_2$ (**1**) has been chosen as the appropriate candidate for such a study, since it resembles a sulfur ylide and can functionalize tailor-made CR_2/NR-transfer reagents. The $[H_2CS(N^tBu)_2]^{2-}$ dianion is an analogue of SO_3^{2-}, in which two oxygen atoms are isoelectronically replaced by a N^{t}Bu imido group and the third one is substituted by a CH_2 carbon group.[9] The sulfur-bonded heteroatom groups form a tridentate ligand.

The coordination of a carbanion to a Li_3 triangle, a structural motif well known all throughout organolithium chemistry, is present in **1**, too.[10] This enables us to study the interactions within this motif for the first time on the basis of an experimental charge density determination. Up to now the bonding mode and the forces that keep the highly charged Li^+ cations together are not fully understood. The gained knowledge should enable chemists to tailor-target organolithium compounds. Furthermore, a better understanding of the reaction behavior, especially of stereochemically active organolithium reagents, can be envisaged.

Polymorphism and Crystal Structure. The attempt to obtaincrystals suitable for a charge density study of [(thf)Li$_2$-{H$_2$CS(N^{t}Bu)$_2$}]$_2$ (**1**) resulted in the discovery of three different polymorphous phases (**1a**, **1b**, **1c**). While the first polymorph of the literature-known modification[7] was determined by routine

* Corresponding author. Phone: (+49)551-39-3000. Fax: (+49)551-39-3459. E-mail: dstalke@chemie.uni-goettingen.de.

(1) (a) Aggarwal, V. K.; Richardson, J. *Chem. Commun.* **2003**, *21*, 2644–2651. (b) Aggarwal, V. K.; Winn, C. L. *Acc. Chem. Res.* **2004**, *37*, 611–620.

(2) (a) Brandt, S. Helquist, P. *J. Am. Chem. Soc.* **1979**, *101*, 6473–6475. (b) Kremer, K. A. M. Helquist, P. Kerber, R. C. *J. Am. Chem. Soc.* **1981**, *103*, 1862–1864. (c) O'Connor, E. J. Helquist, P. *J. Am. Chem. Soc.* **1982**, *104*, 1869–1874. (d) Weber, L. *Angew. Chem.* **1983**, *95*, 539–551; *Angew. Chem., Int. Ed. Engl.* **1983**, *22*, 516–528.

(3) (a) Aggarwal, V. K. *Synlett* **1998**, *4*, 329–336. (b) Tewari, R. S.; Awasthi, A. K.; Awasthi, A. *Synthesis* **1983**, *4*, 330–331. (c) Franzen, V.; Driesen, H.-E. *Chem. Ber.* **1963**, *96*, 1881–1890.

(4) Reuter, P. Ph.D. Thesis, Germany, Bonn, 1986.

(5) Walfort, B.; Leedham, A. P.; Russell, C. R.; Stalke, D. *Inorg. Chem.* **2001**, *40*, 5668–5674.

(6) Walfort, B.; Stalke, D. *Angew. Chem.* **2001**, *113*, 3965–3969; *Angew. Chem., Int. Ed.* **2001**, *40*, 3846–3849. .

(7) Walfort, B.; Bertermann, R.; Stalke, D. *Chem.−Eur. J.* **2001**, *7*, 1424–1430.

(8) Leusser, D.; Henn, J.; Kocher, N.; Engels, B.; Stalke, D. *J. Am. Chem. Soc.* **2004**, *126*, 1781–1793.

(9) (a) Beswick, M. A.; Wright, D. S. *Coord. Chem. Rev.* **1998**, *176*, 373–406. (b) Fleischer, R.; Stalke, D. *Coord. Chem. Rev.* **1998**, *176*, 431–450. (c) Stalke, D. *Proc. Indian Acad. Sci.* **2000**, *112*, 155–170. (d) Brask, J. K.; Chivers, T. *Angew. Chem.* **2001**, *113*, 4082–4098; *Angew. Chem., Int. Ed.* **2001**, *40*, 3960–3976. (e) Aspinall, G. M.; Copsey, M. C.; Leedham, A. P.; Russell, C. R. *Coord. Chem. Rev.* **2002**, *227*, 217–232.

(10) (a) For example ^{t}BuLi and ^{n}BuLi: Kottke, T.; Stalke, D. *Angew. Chem.* **1993**, *105*, 619–621;*Angew. Chem., Int. Ed. Engl.* **1993**, *32*, 580–582. (b) Review: Stey, T.; Stalke, D. Lead structures in lithium organic chemistry. In *The Chemistry of Organolithium Compounds*; Rappoport, Z., Marek, I., Eds.; John Wiley & Sons: Chichester, 2004; pp 47–120.

10.1021/om800046n CCC: $40.75
Publication on Web 04/24/2008

Scheme 1. Possible Reaction Pathways for Sulfur Ylides[a]

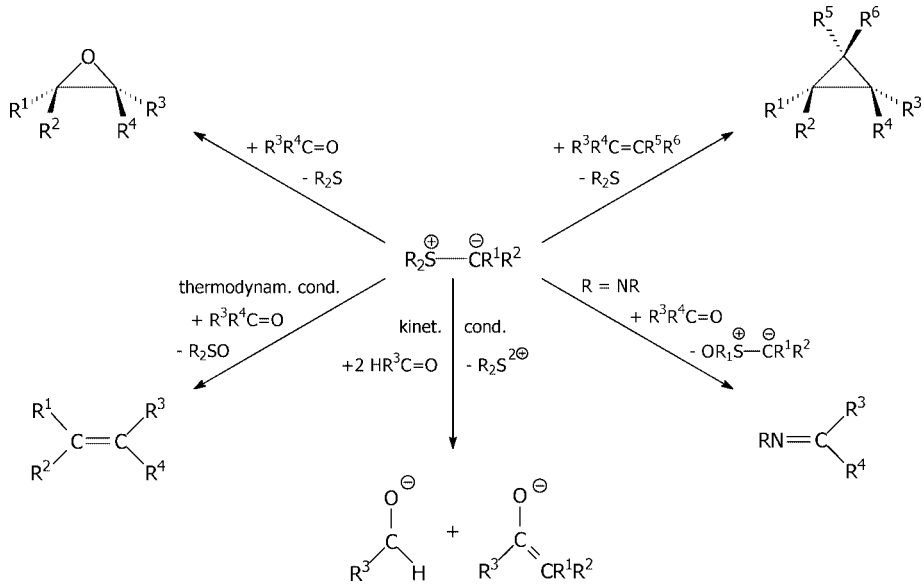

[a] R = alkyl, aryl, imido; R^1, R^2, R^3, R^4 = alkyl, aryl.

Scheme 2. Possible Lewis Formulas for $[(thf)Li_2\{H_2CS(N^tBu)_2\}]_2$ (1): (a) Ylenic Hypervalent Resonance Formula, (b and c) Ylidic but Hypervalent Resonance Formulas, and (d) Ylidic, Non-hypervalent Formula

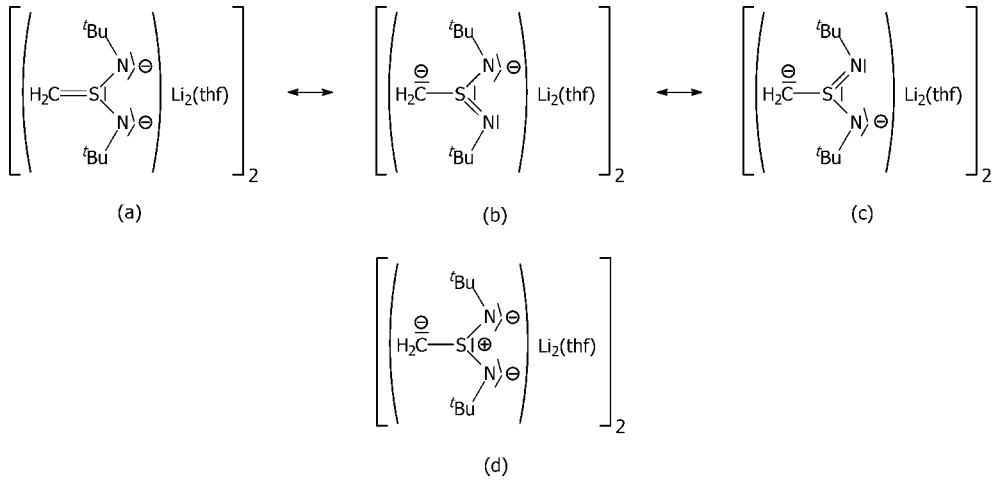

X-ray structure analysis, the second was searched for extensively in order to get a nondisordered low-temperature crystalline phase suitable for a charge density study.[11] The polymorphous transitions could be determined to be of first order, because they are destructive and show superheating/-cooling (determined by DSC).[11,12]

In all polymorphs, $[(thf)Li_2\{H_2CS(N^tBu)_2\}]_2$ (**1**) adopts a dimeric structure by formation of a $S_2N_4C_2Li_4$ double cube (cf. Figure 1a). The two cubes are fused through a Li_2C_2 face. The four ^{t}Bu groups and the two thf donor molecules are bound to the edges of the double cube. The polymorphous transitions can be characterized to be of the displacement type due to the slight shifts in the atomic positions (cf. Figure 2).

The structures of aza and carba sulfites are mainly determined by the preferred environment of the heteroatoms.[7] Thus, the nitrogen atoms are surrounded tetrahedrally by one three-valent sulfur(IV) atom, one tert. carbon atom, and two coordinated lithium atoms. The ylidic carbon atoms, in contrast, adopt an octahedral environment by coordination of three lithium atoms and by bonding of one sulfur and two hydrogen atoms. This leads to the formation of the mentioned double cube. In addition, this is the only way to establish a structural motif well known throughout organolithium chemistry, the carbanion-capped Li_3 triangle (cf. Figure 1).[10] Any other dimerization (e.g. the formation of a Li_4 tetrahedron as in $[(MeLi)_4]$) would result in two Li_3 faces that lack coordination by a carbanion.

The structure of the dimer is very similar in all polymorphs of $[(thf)Li_2\{H_2CS(N^tBu)_2\}]_2$ (**1**), as can be seen from a superpositional plot of the molecules (cf. Figure 2). The central part of the double cube is very rigid, and even the ^{t}Bu groups do not rotate significantly since they adopt a sterically ideal staggered arrangement with respect to the three in-cube bonds of the pivot nitrogen atom (one S−N, two Li−N bonds). The only structural degree of freedom is therefore the torsion of the thf molecules. Because of this similarity, only the structural features of the low-*T* modification **1c** will be discussed. Additionally, both cubes of the dimer are almost equal in **1a**,

(11) More information can be found in the Supporting Information.

(12) Polymorphous transformation energies: **1a** → **1b** −280.1 J/mol, **1b** → **1c** −185.1 J/mol. The figures given should be handled with care because a low-*T* standard (below 173 K) was not available! Nevertheless, the exothermic behavior is clear.

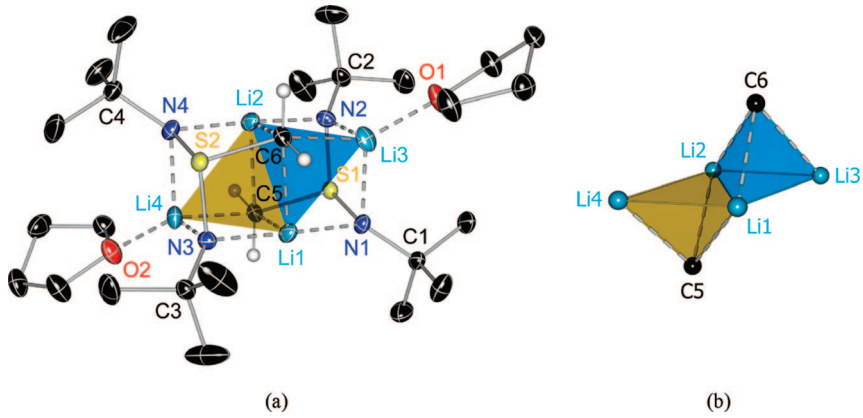

Figure 1. Crystal structure of $[(thf)Li_2\{H_2CS(N^tBu)_2\}]_2$ (**1c**) (a) and Li_3C motif (b).

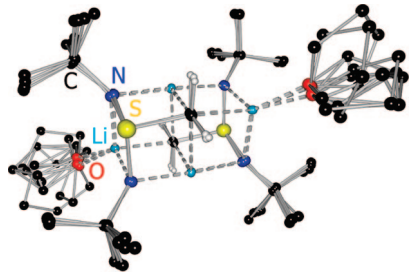

Figure 2. Superposition of all $[(thf)Li_2\{H_2CS(N^tBu)_2\}]_2$ dimers in the polymorphs **1a**, **1b**, and **1c** including all positions of the disordered thf molecules.

1b, and **1c**, and only the thf carbon atoms do not fit the noncrystallographic center of inversion in the middle of the double cube. For this reason, the discussion is limited to one half of the dimer in **1c**, although only **1a** is centrosymmetric.

The S−N bond lengths in $[(thf)Li_2\{H_2CS(N^tBu)_2\}]_2$ (**1**) are almost equal (1.6487(4) and 1.6561(4) Å) and in the range reported for similar compounds, such as $S(NR)_3^{2-}$ and $RS(NR)_2^-$.[7,13] It is worthy to note, that the N−Li bond lengths differ significantly. While N1 forms contacts of 1.9822(8) and 2.1047(9) Å to Li1 and Li3, respectively, the N2−Li bonds are 2.0085(9) (Li2) and 2.0589(9) Å (Li3) in length. Nevertheless, for both nitrogen atoms the contact to the lithium atom in the corner of the cube (Li3) is longer. The S−C bonds are 1.7803(4) Å long and therefore in the range typically quoted for alkyl diazasulfinates[13] and alkyl triazasulfonates[14] (1.79–1.81 Å). Li1, Li2, and Li4 form an isosceles triangle. The Li1···Li2 distance in the common face of the double cube is considerably longer (2.7162(11) Å) than the Li···Li distances including Li4 (2.6315(11) and 2.6496(11) Å). Although the carbanion μ_3-caps the Li_3 triangle, not all C−Li bond distances are equal. C5−Li4 is about 0.11 Å shorter than the other two C−Li contacts (2.3829(9) and 2.40131(9) Å). Thus, the carbanion is shifted away from the hypotenuses closer to the tip of the isosceles Li_3 triangle, which makes the bond to Li4 the preferred coordination. This effect was also observed in the hexameric structure of $[(nBuLi)_6]$.[10a]

Experimental Details. The crystals of **1b** and **1c** were removed from a Schlenk flask under an argon atmosphere and handled in perfluorinated polyether oil under a cold nitrogen gas stream with an X-TEMP2 device to select and prepare a 0.2 × 0.25 × 0.45 mm (**1b**) and a 0.2 × 0.2 × 0.3 mm (**1c**) block-shaped single crystal.[15] Each crystal was mounted on a glass fiber and shock-cooled in the low-temperature gas stream of the diffractometer.

The diffraction data for polymorph **1b** in $P\bar{1}$ were collected at 173 K with Mo K_α radiation ($(\sin\theta/\lambda)_{max} = 0.65$ Å^{-1}, with $R_{int} = 0.0380$ and $R_\Sigma = 0.0289$). The lattice constants were determined to be $a = 10.509(6)$ Å, $b = 11.620(7)$ Å, $c = 15.336(9)$ Å, $\alpha = 110.664(10)°$, $\beta = 92.351(12)°$, $\gamma = 91.119(12)°$.[11]

The diffraction data for polymorph **1c** without disorder were collected at 120 K on a Bruker TXS Mo rotating anode with INCOATEC Helios mirror optics and an APEX II detector. The data were recorded in a low-order and high-order batch. This procedure led to high-resolution data ($(\sin\theta/\lambda)_{max} = 1.14$ Å^{-1}) at redundancies of more than 18 with a completeness of 100% to $\sin\theta/\lambda = 1.09$ Å^{-1} and 99.8% for the overall data ($R_{int} = 0.0364$ and $R_\Sigma = 0.0154$; at $\sin\theta/\lambda = 0.60$ Å^{-1} like for a routine structure $R_{int} = 0.0262$ and $R_\Sigma = 0.0053$ and $\sin\theta/\lambda = 0.65$ Å^{-1} like **1b** $R_{int} = 0.0284$ and $R_\Sigma = 0.0056$). The unit cell constants were determined to be $a = 17.5816(11)$ Å, $b = 17.5311(11)$ Å, $c = 22.0092(13)$ Å, $\alpha = \beta = \gamma = 90°$.[11]

Refinements. The refinement of **1b** is described in the Supporting Information. For **1c** only a brief statement will be given in this paragraph. The Supporting Information contains a detailed description of the refinement procedure.

An IAM served as starting model for the subsequent multipole refinements of **1c** using the atom-centered multipole model by Hansen and Coppens[16] implemented in the XD2006 package.[17]

For the deformation density terms single-ζ orbitals with energy-optimized Slater exponents were used. In the pseudoatom model of the sulfur atoms optimized n_l values (4, 4, 6, 8 for $l = 1, 2, 3, 4$) were selected for the deformation density model.[8,18,19] Several models, differing in the degree of applied

(13) (a) Hänssgen, D.; Steffens, R. *J. Organomet. Chem.* **1982**, *236*, 53–60. (b) Hänssgen, D.; Steffens, R. *Z. Naturforsch.* **1985**, *40b*, 919–922. (c) Pauer, F.; Stalke, D. *J. Organomet. Chem.* **1991**, *418*, 127–128. (d) Pauer, F.; Rocha, J.; Stalke, D. *J. Chem. Soc., Chem. Commun.* **1991**, *20*, 1477–1479. (e) Edelmann, F. T.; Knösel, F.; Pauer, F.; Stalke, D.; Bauer, W. *J. Organomet. Chem.* **1992**, *438*, 1–10. (f) Freitag, S.; Kolodziejski, W.; Pauer, F.; Stalke, D. *J. Chem. Soc., Dalton Trans.* **1993**, 3479–3488.

(14) (a) Appel, R.; Kohnke, J. *Chem. Ber.* **1971**, *104*, 3875–3883. (b) Fleischer, R.; Walfort, B.; Gbureck, A.; Scholz, P.; Kiefer, W.; Stalke, D. *Chem.−Eur. J.* **1998**, *4*, 2266–2279.

(15) (a) Stalke, D. *Chem. Soc. Rev.* **1998**, *27*, 171–178. (b) Kottke, T.; Stalke, D. *J. Appl. Crystallogr.* **1993**, *26*, 615–619.

(16) Hansen, N. K.; Coppens, P. *Acta Crystallogr.* **1978**, *A34*, 909–921.

(17) Volkov, A.; Macchi, P.; Farrugia, L. J.; Gatti, C.; Mallinson, P. R.; Richter, T.; Koritsanszky, T. *XD2006A Computer Program Package for Multipole Refinement, Topological Analysis of Charge Densities and Evaluation of Intermolecular Energies from Experimental or Theoretical Structure Factors*; 2006.

(18) (a) Leusser, D. Walfort, B. Stalke, D. *Angew. Chem.* **2002**, *114*, 2183–2186; *Angew. Chem., Int. Ed.* **2002**, *41*, 2079−2082.

chemical constraints and local non-crystallographic symmetry have been refined and compared. The model that led to the lowest *R* values, the lowest standard deviations, and a flat and featureless residual density at minimal correlations was selected for the following discussion. It was tested if the stabilizing constraints in the final model keep it flexible enough to model small differences of the chemically equivalent subunits of the molecule.

Special care was taken to account for the electronic state of the lithium atoms. Three different models have been compared for them: (i) neutral lithium atom with one electron in the valence shell, which was modeled by a monopole function and scaled by κ; (ii) Li^+scattering factor for all lithium atoms as starting model (no monopole); (iii) Li^+ scattering factor for all lithium atoms; in the first step the four valence electrons of the four Li^+ were distributed over the bonded nitrogen atoms. All refined models led to a converged fit at low *R* values with flat and featureless residual densities and similar density properties. In detail, model i revealed almost zero monopole populations for the lithium atoms and a severe contracted scattering factor (large κ). Therefore model ii or iii seemed to be appropriate to describe the scattering of the lithium atoms. For electroneutrality reasons model iii was favored, even more since the comparison with ii did not reveal severe net charge differences at the nitrogen atoms after the refinement. This showed that the charge distribution at the nitrogen centers was not predetermined by the starting model, but was straightforward concerning chemical electroneutrality.

The multipole refinement led to a very satisfactory fit. This is reflected in the low *R* values, flat and featureless residual densities, and low standard deviations of the refined parameters at low correlations.[20]

Topological Analysis and Laplacian Distribution. To obtainmore insight into the bonding situation of $[(thf)Li_2\{H_2CS(N^tBu)_2\}]_2$ (**1c**), a detailed topological analysis according to Bader's quantum theory of atoms in molecules (QTAIM) was performed.[21] (3,−1) bond critical points (BCPs) in $\rho(\mathbf{r})$ representing saddle points in the density distribution between two atoms were determined for all anticipated bonds as well as the resulting ring (RCPs, (3,+1)) and a cage critical point (CCP, (3,+3)) in the center of the double cube (cf. Figure 3). The number of critical points determined fulfills the Poincaré-Hopf equation and is therefore self-consistent (for details see the Supporting Information).

The values of the charge densities, $\rho(\mathbf{r}_{BCP})$, and the Laplacians, $\nabla^2\rho(\mathbf{r}_{BCP})$, at the BCPs of **1c** are presented in Table 1. According to the QTAIM, a bond path is a sufficient and necessary condition of a chemical bond[22] and the properties at the BCP can be used to distinguish between various types of atomic interactions. Negative values of the Laplacian accompanied by high values of the density at the BCP are commonly associated with a distinct covalent character of the bond (*shared interactions*), while highly positive values in the Laplacian accompanied by relatively small values of the electron density are attributed to an ionic character of the bond (*closed-shell interactions*). However, it is well known that this strict classification does not hold for very polar bonds or interactions with or between metal atoms.[8,23,24] Nevertheless, since the BCP is defined as the local minimum along a path of maximum density between two bound atoms, the BCP properties should correlate at least for different bonds made up by the same atom types. Indeed, as can be seen from Table 1, significant differences of the C−Li and N−Li bonds can be observed.

In addition, we investigated the second derivative of the charge density distribution, $\nabla^2\rho(\mathbf{r})$, which represents charge accumulations and depletions, and determined the anticipated valence shell charge concentrations (VSCCs) appearing as (3, −3) critical points in the negative Laplacian (local maximum) and the values of the local charge concentrations (CCs) in $-\nabla^2\rho(\mathbf{r}_{CC})$. The correlation between these values, which originate from bonding (BCCs) or non-bonding charge concentrations (NBCCs), often referred to as lone pairs (LPs), on one hand, and the anticipated bond strength in **1c**, on the other hand, is remarkable (cf. Figure 1 and Table 1). Other intriguing features are the angles between the CCs (cf. Table 2), which

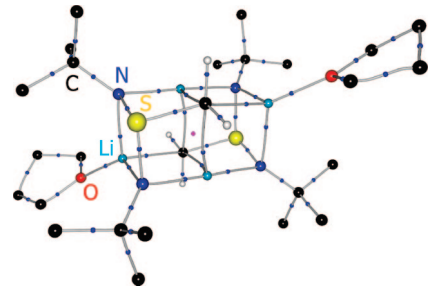

Figure 3. Graphical representation of the bond paths along the chemical connectivities, BCPs, and CCP in $[(thf)Li_2\{H_2CS(N^tBu)_2\}]_2$ (**1c**).[33] Blue spheres represent positions of BCPs, where a magenta one denotes the CCP in the center of the double cube. RCPs are omitted for clarity.

Table 1. BCP Properties of $[(thf)Li_2\{H_2CS(N^tBu)_2\}]_2$ (1c)[a]

	d_{geom}	$d_{bond\ path}$	d_{BCP}	$\rho(\mathbf{r}_{BCP})$	$\nabla^2\rho(\mathbf{r}_{BCP})$
S1−N1	1.6487(4)	1.65057	0.7600	1.670(19)	−11.518(56)
S1−N2	1.6561(4)	1.65952	0.6902	1.547(22)	−9.774(70)
S1−C5	1.7803(4)	1.78210	0.9858	1.369(12)	−5.214(28)
C5−Li1	2.4013(9)	2.42446	1.55796	0.078(1)	+1.663(1)
C5−Li2	2.3829(9)	2.40134	1.54375	0.080(1)	+1.747(1)
C5−Li4	2.2753(8)	2.28786	1.47602	0.107(1)	+2.299(1)
N1−C1	1.4763(6)	1.47776	0.8211	1.875(9)	−12.959(31)
N2−C2	1.4726(6)	1.47424	0.8070	1.835(9)	−10.675(30)
N1−Li1	1.9822(8)	1.98375	1.2531	0.201(2)	+5.166(2)
N1−Li3	2.1047(9)	2.10880	1.3280	0.129(2)	+3.580(1)
N2−Li2	2.0085(9)	2.01200	1.2726	0.187(2)	+4.905(2)
N2−Li3	2.0589(9)	2.06042	1.2991	0.154(2)	+3.994(2)
O1−Li3	1.9472(9)	1.94745	1.2002	0.150(2)	+5.110(2)
O2−Li4	1.9492(9)	1.94964	1.2025	0.151(2)	+5.053(2)
C5−H101	1.0850(4)	1.08520	0.7426	1.655(16)	−15.076(55)
C5−H102	1.0850(4)	1.08518	0.7425	1.654(8)	−15.077(22)

[a] d_{geom} is the geometrical bond length [Å], $d_{bond\ path}$ is the bond path length [Å], d_{BCP} [Å] denotes the distances of the BCP from the first atom, $\rho(\mathbf{r}_{BCP})$ [e/Å^3] is the charge density, and $\nabla^2\rho(\mathbf{r}_{BCP})$ [e/Å^5] is the Laplacian at the BCP.

(19) Dominiak, P. M.; Coppens, P. *Acta Crystallogr.* **2006**, *A62*, 224–227.

(20) Residuals after multipole refinement: $wR_1(I > 3\sigma(I)) = 0.0248$, $wR_2(I > 3\sigma(I)) = 0.0489$, $w = 1/\sigma^2$, GoF = 4.0636 (affected by the use of the $1/\sigma^2$-weighting scheme) $N_{refl}/N_{param} = 39$. The final difference Fourier synthesis led to a flat and featureless distribution ($\rho_{res.,max} = 0.41$ e/Å^3, $\rho_{res.,min} = -0.53$ e/Å^3 to $(\sin\theta/\lambda)_{max} = 1.00$ Å^{-1} and $\rho_{res.,max} = 0.30$ e/Å^3, $\rho_{res.,min} = -0.37$ e/Å^3 to $(\sin\theta/\lambda)_{max} = 0.80$ Å^{-1}). The 10 most distinct maxima and minima with a cut-off at $(\sin\theta/\lambda)_{max} = 0.80$ Å^{-1} were found around the ^{t}Bu groups. Therefore they should not affect the discussed features significantly.

(21) Bader, R. F. W. *Atoms in Molecules−A Quantum Theory*; Oxford University Press: New York, 1990.

(22) (a) Bader, R. F. W. *J. Phys. Chem.* **1998**, *A102*, 7314–7323. (b) Henn, J.; Leusser, D.; Stalke, D. *J. Comput. Chem.* **2007**, *28*, 2317–2324.

(23) Kocher, N.; Henn, J.; Gostevskii, B.; Kost, D.; Kalikhman, I.; Engels, B.; Stalke, D. *J. Am. Chem. Soc.* **2004**, *136*, 5563–5568.

(24) Henn, J.; Ilge, D.; Leusser, D.; Stalke, D.; Engels, B. *J. Phys. Chem.* **2004**, *A108*, 9442–9452.

Table 2. Bond Angles Calculated from the Atomic Positional Parameters and Angles Made up by the CCs of [(thf)Li$_2${H$_2$CS(N^{t}Bu)$_2$}]$_2$ (1c)[a]

	bond angle	CC angle		bond angle	CC angle
N1−S1−N2	103.97(2)°		S1−N1−C1	116.26(3)°	
$CC_{S1\rightarrow N1}$−S1−$CC_{S1\rightarrow N2}$		107.5°	$CC_{N1\rightarrow S1}$−N1−$CC_{N1\rightarrow C1}$		101.9°
C5−S1−N1	99.30(2)°		S1−N1−Li1	99.98(3)°	
$CC_{S1\rightarrow C5}$-S1−$CC_{S1\rightarrow N1}$		106.9°	$CC_{N1\rightarrow S1}$-N1−$LP_{N1\rightarrow Li1}$		107.7°
C5−S1−N2	100.31(2)°		S1−N1−Li3	88.62(3)°	
$CC_{S1\rightarrow C5}$−S1−$CC_{S1\rightarrow N2}$		102.2°	$CC_{N1\rightarrow S1}$−N1−$LP_{N1\rightarrow Li3}$		116.1°
N1−S1−LP	–		C1−N1−Li1	135.59(4)°	
$CC_{S1\rightarrow N1}$−S1−LP_{S1}		107.3°	$CC_{N1\rightarrow C1}$−N1−$LP_{N1\rightarrow Li1}$		135.2°
N2−S1−LP	–		C1−N1−Li3	122.88(4)°	
$CC_{S1\rightarrow N2}$−S1−LP_{S1}		108.6°	$CC_{N1\rightarrow C1}$−N1−$LP_{N1\rightarrow Li3}$		106.9°
C5−S1−LP	–		Li1−N1−Li3	80.39(3)°	
$CC_{S1\rightarrow C5}$−S1−LP_{S1}		123.4°	$LP_{N1\rightarrow Li1}$−N1−$LP_{N1\rightarrow Li3}$		89.5°
S1−C5−H101	104.16(3)°		S1−N2−C2	116.54(3)°	
$CC_{C5\rightarrow S1}$−C5−$CC_{C5\rightarrow H101}$		110.9°	$CC_{N2\rightarrow S1}$−N2−$CC_{N2\rightarrow C2}$		105.7°
S1−C5−H102	103.52(3)°		S1−N2−Li2	98.40(3)°	
$CC_{C5\rightarrow S1}$−C5−$CC_{C5\rightarrow H102}$		110.7°	$CC_{N2\rightarrow S1}$−N2−$CC_{N2\rightarrow Li2}$		108.1°
H101−C5−H102	106.47(4)°		S1−N2−Li3	90.00(3)°	
$CC_{C5\rightarrow H101}$−C5−$CC_{C5\rightarrow H102}$		104.6°	$CC_{N2\rightarrow S1}$−N2−$CC_{N2\rightarrow Li3}$		92.4°
S1−C5−LP	–		C2−N2−Li2	128.35(4)°	
$CC_{C5\rightarrow S1}$−C5−LP_{C5}		101.9°	$CC_{N2\rightarrow C2}$−N2−$CC_{N2\rightarrow Li2}$		113.4°
H101−C5−LP	–		C2−N2−Li3	132.22(4)°	
$CC_{C5\rightarrow H101}$−C5− LP_{C5}		114.3°	$CC_{N2\rightarrow C2}$−N2−$CC_{N2\rightarrow Li3}$		118.1°
H102−C5−LP	–		Li2−N2−Li3	80.62(3)°	
$CC_{C5\rightarrow H102}$−C5− LP_{C5}		114.6°	$CC_{N2\rightarrow Li2}$−N2−$CC_{N2\rightarrow Li3}$		115.8°

[a] $CC_{i\rightarrow j}$ denotes the charge concentrations at atom i in the direction of atom j, $LP_{i\rightarrow j}$ a lone pair at atom i in the direction of atom j, LP_i a NBCC at atom i or a Li_3-face directed lone pair.

can serve as an alternative interpretation for bond angles, since they represent the bond-induced CCs of the atomic valence shells and are therefore the charge density analogue to the geometry-based bond angles of Table 2.

Since the atomic densities of the [Li$_2${H$_2$CS(N^{t}Bu)$_2$}]$_2$ unit have been modeled under the assumption of chemical constraints, which are postulated by a molecular non-crystallographic inversion center in the midpoint of the molecule, we discuss just one of the structurally and electronically independent [Li$_2${H$_2$CS(N^{t}Bu)$_2$}] fragments.[25]

From the charge density point of view the [H$_2$CS(N^{t}Bu)$_2$] dianion is unequivocally the most interesting part of the molecule. In our earlier work we focused on the question of how formal A═B (A = S, P, Si and E = F, O, N, C) bonds in so-called hypervalent species should be described: as A═B double bonds or as an A^+-B^- type of interaction.[8,18,26] Up to now, we found the A^+-B^- type to be the electronically appropriate interpretation for all compounds under investigation. In this context the [H$_2$CS(N^{t}Bu)$_2$] ligand gives rise to two questionable bond types, S═N versus S^+-N^- and S═C versus S^+-C^-.

S−N and S−C Bonds. Comparing the BCP properties of the present S−N bonds with the ones published before, we find the bonding situation in perfect agreement with the S−N bonds in H(N^{t}Bu)$_2$SMe and CH$_2${(N^{t}Bu)$_2$H(N^{t}Bu)}$_2$.[8] The bond lengths and the topological properties at the BCPs do not differ more than about 10% ($\rho(\mathbf{r}_{BCP})$) to 20% ($\nabla^2\rho(\mathbf{r}_{BCP})$) compared to the values given there for the single-bonded nitrogen atoms (cf. Table 1). Hence, there should be no doubts about the presence of an S^+-N^- type of interaction: four VSCCs at the sulfur atom are present (cf. Figure 4). Three of them are directed toward the bound neighbors N1, N2, and C5, and one NBCC is oriented as expected for a sp^3-hybridized sulfur atom.

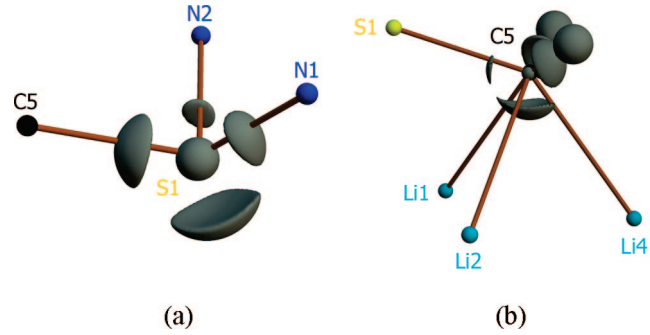

Figure 4. Isosurface representation of the VSCCs at S1 (a) and C5 (b). Isosurfaces values: (a) −9 e/Å^5 and (b) −16 e/Å^5.

The VSCCs around the sulfur atom include angles that are much closer to the ideal tetrahedral angles than the plain connectivity-related angles suggest (cf. Table 2). They range from 102.2° ($CC_{S1\rightarrow C5}$−S1−$CC_{S1\rightarrow N2}$) to 107.5° ($CC_{S1\rightarrow N1}$−S1−$CC_{S1\rightarrow N2}$), compared with 100.31° to 103.97° for the equivalent values resulting from straight line atom connectivities. Additional to the BCC-based angles, the topological analysis allows the determination of the lone-pair angles at the sulfur atom. They are very close to the ideal value (107.3° for $CC_{S1\rightarrow N1}$−S1−LP_{S1} and 108.6° for $CC_{S1\rightarrow N2}$−S1−LP_{S1}) except for $CC_{S1\rightarrow C5}$−S1−LP_{S1}, which is significantly widened to 123.4°. This dilated angle is in perfect agreement with the predictions from VSEPR theory,[27] since the charge concentration of the LP is the most distinct one with −18.1 e/Å^5, followed by the CC toward C5 with −15.9 e/Å^5, while the nitrogen-directed CCs are less pronounced ($CC_{S1\rightarrow N2}$ = −10.6, $CC_{S1\rightarrow N1}$ = −12.9 e/Å^5). Therefore, it is not surprising that the spatial demand of LP_{S1} and the relatively high $CC_{S1\rightarrow C5}$ leads to an increase of the enclosed angle. The integrated charge of the sulfur atoms is +0.87*e*, while the net charge is +0.12*e*, suggesting the local positive charge at S1 to originate mainly

(25) The topological properties have been determined for both halves, but no significant differences have been detected (they predominately arise from those groups that do not fulfill this symmetry restriction, e.g. the two thf molecules).

(26) Kocher, N.; Leusser, D.; Murso, A.; Stalke, D. *Chem.−Eur. J.* **2004**, *10*, 3622–3631.

(27) Chemical Bonding and Molecular Geometry. In *Chemical Bonding and Molecular Geometry*; Gillespie, R. J., Popelier, P. L. A., Eds.; Oxford University Press: New York, 2001.

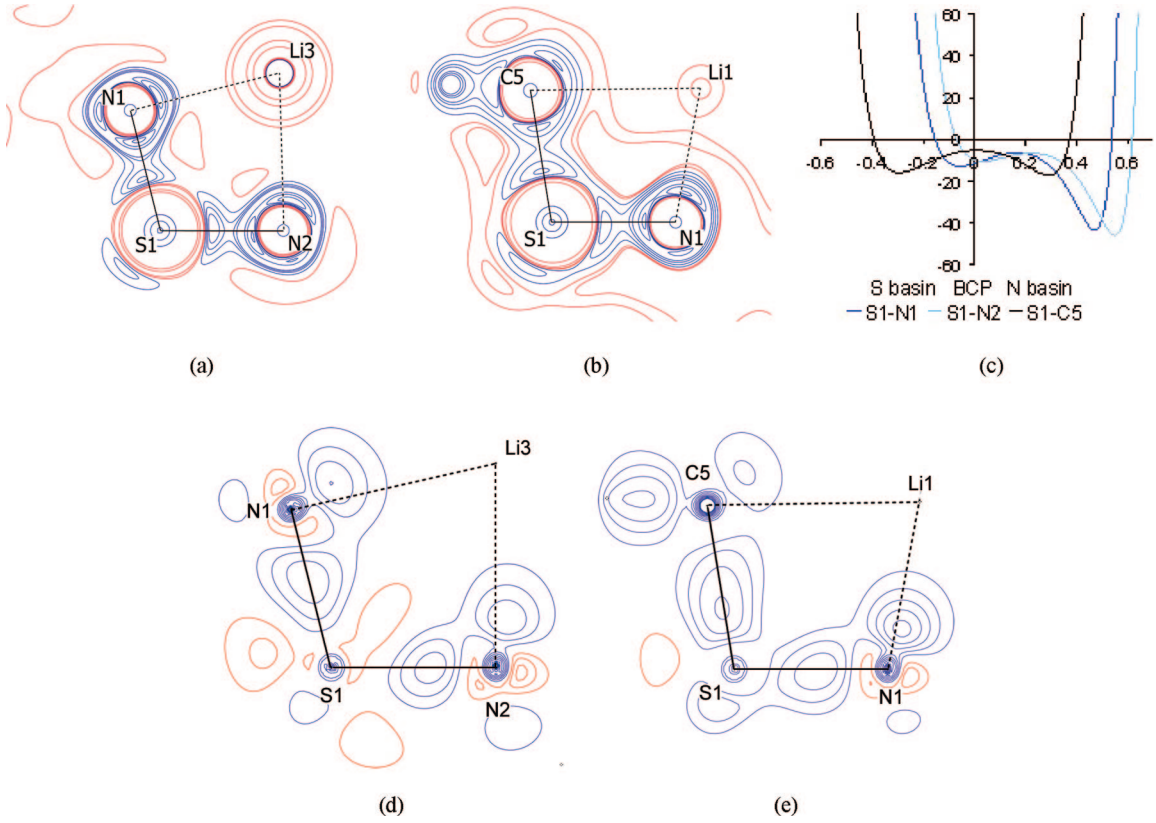

Figure 5. $\nabla^2\rho(\mathbf{r})$ distributions in the S1N1N2 (a) and S1N1C5 (b) planes and along the S−N and S−C bond paths (c). Contour plots (a) and (b): $\nabla^2\rho(\mathbf{r})$, blue contours show negative values (electron density concentrations), red contours positive ones (electron density depletions); plots (d) and (e): deformation density, blue contours show positive values, red contours negative ones (step size 0.1 e/Å^3); profile plot c: $\nabla^2\rho(\mathbf{r})$ [e/Å^5] along the S−N and S−C bond paths (*x*-axis: distance from the BCP).

from polarization effects.[11] The topological analysis allows to determine physically meaningful charges by integrating the electron density over the atomic basins, separated by the zero-flux condition $\nabla\rho(\mathbf{r})\cdot n(\mathbf{r}) = 0$. These charges originate from bond *polarization* effects as well as *charge transfer* between the atomic centers. They should be compared to the atomic *net charges*, which are calculated from the difference of the number of valence electrons and the monopole populations of an atom (see Table 3 of the Supporting Information). Therefore those charges result solely from an electron density shift between atoms within the refinement routine, and they account for atomic *charge transfer* in the molecule.

Although chemically equivalent, the S−N bonds reveal different charge density features, which are already reflected by the different values of the bond-related CCs at S1. Even though the S−N bond path lengths differ less than 0.01 Å (S1−N1 = 1.65057 Å, S1−N2 = 1.65952 Å), the topological features at the BCPs differ significantly.

The density at the BCP is about 10% higher for S1−N1 (1.670 vs 1.547 e/Å^3) compared to S1−N2, guided by a more negative value for $\nabla^2\rho(\mathbf{r}_{BCP})$ (−11.518 vs −9.774 e/Å^5) but a much less pronounced ellipticity of the bond density (0.07 and 0.30). This might be caused by a shift of the BCP in the S1−N1 bond toward N1 compared to S1−N2, leading to an increased atomic basin of N2 in the direction of S1, which is reflected in the higher integrated charge (−1.21*e* for N2 vs. −1.14*e* for N1). On the other hand the overall atomic volumes of the nitrogen atoms defined by their zero-flux surfaces do not differ significantly (14.25 and 14.16 Å^3), which makes a counterbalancing effect necessary. The N−^{t}Bu contacts can be ruled out to be responsible for that (cf. Table 1), since they are almost equal concerning all density-related properties ($\rho(\mathbf{r}_{BCP})$, $\nabla^2\rho(\mathbf{r}_{BCP})$) as well as the atomic properties of the tertiary carbon atoms (charge, atomic volume). Just the BCP is slightly closer to N2 compared to N1−C1 at equal bond path lengths. Therefore, the differences between the two S−N bonds should be induced or at least reflected by the N−Li contacts. Both nitrogen atoms bind to Li3. We find the N1−Li3 path about 0.05 Å elongated (2.10880 and 2.06042 Å) with the BCP more than 0.02 Å closer to Li3 and a 20% reduced $\rho(\mathbf{r}_{BCP})$ (0.129 and 0.154 e/Å^3) compared to N2. The opposite effect is found for the two remaining nitrogen−lithium contacts, N1−Li1 and N2−Li2: the first is 0.03 Å shorter, the associated BCP 0.02 Å closer to N1, and $\rho(\mathbf{r}_{BCP})$ about 10% higher. Interestingly, these effects are echoed by the values of the VSCCs at the nitrogen atoms. We found four BCCs at each nitrogen atom, all of them oriented toward the anticipated bonding partner (see Figure 5a,b). The $CC_{N2\rightarrow S1}$ is inclined out of the SN_2 triangle, while the $CC_{N1\rightarrow S1}$ is aligned along the N1−S1 vector. The corresponding CCs at S1 show an inverse distribution: $CC_{S1\rightarrow N1}$ points outward and $CC_{S1\rightarrow N2}$ is oriented along the straight connection line between the two atoms.

The Laplacian distributions along the S−N bond paths (cf. Figure 5c) display the shape of a severely polarized shared interaction. At S1, as well as N1 and N2, minima are established and the distribution is negative over the whole bonding region. The polarization can be deduced from the positions of the BCPs, which are located very close to the charge concentration of S1 and from the absolute value of the minima, which are about doubled for the nitrogen atoms compared to the sulfur atom. The different topological properties at the S−N BCPs are also reflected in the shape of the Laplacian distributions along the

bond paths. The two distributions are qualitatively equal but shifted parallel with respect to the *y*-axis (cf. Figure 5c). This is a well-known observation for bonds of the same type but of different lengths. However, the identical S−N bond lengths allow the conclusion that the individual distributions refer to individual topologies.

Taking into account the similarity to the S^+-N^- bonds in $H(N^tBu)_2SMe$ and $CH_2\{(N^tBu)_2(N(H)^tBu)\}_2$[8] and the integrated charges as well as the net charges of the nitrogen atoms (N1 = −1.14/−0.54*e*, N2 = −1.21/−0.56*e*), which imply a notable contribution to the charge to originate from a charge transfer,[11] we assume the nitrogen atoms to be negatively charged. The 4-fold coordination is made up by the two single bonds to the sulfur and the tertiary carbon atom and guided by two lone-pair-driven N^-Li^+ bonds. Around N1 we determined the most distinct charge concentrations oriented toward Li1 (−59.6 e/Å^5) and Li3 (−51.3 e/Å^5) and the less pronounced to S1 (−44.8 e/Å^5) and C1 (−48.9 e/Å^5). Around N2, which seems to polarize the sulfur atom and Li2 even more, the associated BCCs are increased compared to N1 (−64.9 to Li2, −52.7 to Li3, −46.1 to S1, and −43.0 e/Å^5 to C2).

For the N−Li Laplacian distributions along the bond paths two groups can be distinguished. The shorter bonds (N1−Li1, N2−Li2) reveal more pronounced minima compared to the N−Li bonds to the corner of the cube. The asymmetry of the nitrogen basins mentioned above, which was also present in the Laplacian distribution of the SN_2 plane, is reflected in the N−Li bonds. While the minimum of N1−Li3 is shifted away from the BCP toward N1 compared to N2−Li3, the minimum of N1−Li1 is shifted toward the BCP compared to N2−Li2.

The asymmetric charge density distribution in the SN_2 backbone and its impact on the N^-Li^+ bonds also influence the S−C as well as the C−Li interaction.

Independently from the fine-graded density features of the two chemically equivalent but electronically distinguishable S−N bonds discussed above, the question remains whether the S−C contact should be regarded as a S−C single or S═C double bond. From the charge density point of view this question can be answered straightforwardly: S−C is a standard single bond. The bond path length (1.78210 Å), the charge density, and the Laplacian at the BCP (1.369 e/Å^3, −5.214 e/Å^5) fit the findings in our previously investigated model compounds[8] and other published S−C contacts[8,18,28] perfectly. In contrast to the polar bonds discussed above (S−N, N−Li), the Laplacian distribution along the bond path is almost symmetric. The minima at S1 and C5 are equal in the absolute values. The Laplacian stays negative over the whole bonding region with a local maximum at the BCP, indicating shared interactions. The polarization of the S−C bond is therefore solely reflected in the position of the BCP, which is shifted 0.03 Å away from the nonpolar midpoint (expected position given by the ratio of the covalent radii) toward C5. Thus, the polarization of the S−C bond is remarkably small. The polarization of the S1 valence shell seems to be restricted to the interaction with the more electronegative nitrogen atoms.

This, together with the unambiguously determined lone pair at the sulfur atoms and four VSCCs (one LP and three BCCs) at each of the ylidic carbon atoms (*vide infra*), let us state that the two S−C contacts are undoubtedly S−C single bonds. Again, a hypervalent sulfur species can be ruled out, and thus the resonance formula (d) in Scheme 2 describes the electronic features of **1** best.

Besides the bonding situation in the SN_2C backbone of $[(thf)Li_2\{H_2CS(N^tBu)_2\}]_2$ (**1**), which is related to the question of hypothetical hypervalency of the sulfur atom, the nature of the bonding between the Li^+ atoms and their electronegative neighbors (N, O), on one hand, and the interaction of the Li_3 triangles with the ylidic carbon atoms C5 and C6, on the other hand, are of striking interest. Carbon-capped Li_3 triangles are one of the main structural motifs in lithium organic compounds.[10] The driving forces, which keep these highly charged units together, are still not fully understood and are under debate.[29] It is still an open question to what extent the C−Li contacts can be regarded as purely ionic or with prominent covalent contributions. To our own surprise, the topological features of the compound presented here give very evident and quantified insight into this type of interaction.

C−Li and Li−O Interactions. The lithium atoms in the joint plane of the two face-fused $[Li_2\{H_2CS(N^tBu)_2\}]$ cubes are coordinated by two nitrogen atoms, each of one cube, and by both ylidic carbon atoms. The lithium atoms on the edges (Li3 and Li4) are surrounded by two nitrogen atoms of the associated cube, one ylidic carbon atom, and an oxygen atom of the coordinating thf molecule. The Li−N bonds have been already discussed in the SN_2 section. The Li−O bonds fit our previously investigated lithium donor contacts well. The Li3−O1 bond path and the topological properties at the BCP are in the expected range (1.94745 Å, $\rho(\mathbf{r}_{BCP}) = 0.150$ e/Å^3, $\nabla^2\rho(\mathbf{r}_{BCP}) = +5.110$ e/Å^5). We identified four VSCCs around the oxygen atom, two BCCs formed by the covalent bonds to the carbon atoms in the thf (CC_{C51}: −111.9 e/Å^5 and CC_{C54}: −119.3 e/Å^5) and two LP-associated CCs directed toward Li3 (−122.3 and −122.7 e/Å^5). This bifurcated coordination of an electropositive counterpart by two lone pairs is a well-known feature we already observed in inter- as well as intramolecular $N^-\cdots H$ hydrogen bonds[8] and $Li^+-O_{Et_2O}$[26] and Li^+-O_{thf}[30] contacts. Apart from the coordination mode, the values obtained at the (3,−3) critical points of the Laplacian field (VSCCs) seem to be a measure of the bond strengths of our investigated Li^+-O contacts. The maxima we find in $[(thf)Li_2\{H_2CS(N^tBu)_2\}]_2$ (**1**) are more pronounced than those for $Li^+-O_{Et_2O}$ (−105 e/Å^5) but in the range of the other Li^+-O_{thf} contact (−125 e/Å^5).[31] This is in good agreement with chemical intuition, which expects thf (dipole moment $\mu = 1.75$ D) to have a stronger donor capacity compared to Et_2O ($\mu = 1.15$ D).[32]

Much less is known about the experimental charge density distribution of ylidic carbanions that form the frequently observed Li_3-C_α motif, in which the carbanion μ_3-bridges a Li_3 triangle. In **1** each CH_2 unit caps a Li_3 triangle and forms a tetrahedron, made up of two almost equivalent (C5−Li1, C5−Li2) and one short C−Li contact (C5−Li4). We found the three expected bond paths between C5 and S1, H101, and H102 with the typical density features of these kinds of bonds (cf.

(28) (a) Dahaoui, S.; Pichon-Pesme, V.; Howard, J. A. K.; Lecomte, C. *J. Phys. Chem.* **1999**, *A103*, 6240–6250. (b) Espinosa, E.; Molins, E.; Lecomte, C. *Phys. Rev.* **1997**, *B56*, 1820–1833. (c) Pillet, S.; Souhassou, M.; Pontillon, Y.; Caneschi, A.; Gatteschi, D.; Lecomte, C. *New J. Chem.* **2001**, *25*, 131–143.

(29) (a) Bickelhaupt, F. M.; Solà, M.; Guerra, C. F. *J. Chem. Theory Comput.* **2006**, *2*, 965–980. (b) Matito, E.; Poater, J.; Bickelhaupt, F. M.; Solà, M. *J. Phys. Chem.* **2006**, *B110*, 7189–7198.

(30) Kocher, N.; Selinka, C.; Leusser, D.; Kost, D.; Kahlikhman, I.; Stalke, D. *Z. Anorg. Allg. Chem.* **2004**, *630*, 1777–1793.

(31) In ref 30 another Li-directed CC at an oxygen atom is present with −135 e/Å^5, although this CC results from a disordered thf and was therefore not cited for comparison purposes.

(32) *CRC Handbook of Chemistry and Physics*, 87th ed.; Lide, D. R., Ed.; Taylor & Francis: Boca Raton, 2006.

(33) All remaining CPs are shown in Figure 4 of the Supporting Information and are discussed there.

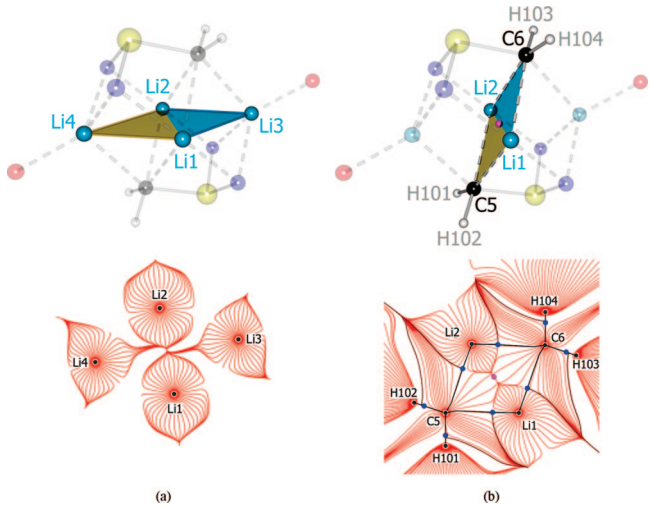

Figure 6. Trajectory plots of the mean Li_4 plane (a) and the central $Li_2(CH_2)_2$ plane (b). In the trajectory plots black solid lines denote bond paths; the BCPs are marked by blue spheres, the CCP by a magenta sphere.

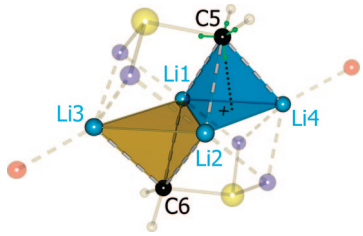

Figure 7. Orientation of the VSCCs at C6. Green spheres denote the positions of the VSCCs; the black cross marks the center of the Li_3 triangle.

Table 1). In addition we detected bond paths, the *necessary* and *sufficient* condition for a bond,[22a] between C5 and all three lithium atoms of the corresponding triangle. In this respect we have to regard the carbon atoms C5 and C6 as 6-fold coordinated. No bond paths could be determined for any of the potential Li···Li contacts (cf. Figure 6); thus no chemical Li−Li bonds should be formulated in the framework of QTAIM.

The integrated charges of C5 and C6, which were determined to be $-0.78e$ each, and their even more distinct net charge of $-0.89e$ support the interpretation of the CH_2 unit as *ylidic*. This is straightforward to the existence of a lone pair, which could be undoubtedly characterized by a VSCC with a value of −23.0 e/Å^5 at the (3,−3) critical point in the negative Laplacian field, $-\nabla^2\rho(\mathbf{r})$. This LP density is inclined toward the closer lithium atom (see Figure 7, Figure 8a,b), which can be quantified by the shortened Li−LP distance (Li4−LP_{C5} = 1.884 Å, Li1−LP_{C5} = 2.071 Å, Li2−LP_{C5} = 2.074 Å) and the wider Li−LP−C angle (Li4−LP_{C5}−C5 = 138.5°, Li1−LP_{C5}−C5 = 127.3°, Li2−LP_{C5}−C5 = 123.8°). Together with the additional three BCCs formed by the polarized, but covalent bonds to S1 (−17.3 e/Å^5), H101 and H102 (−25.0 e/Å^5), this leads to an sp^3-hybridized ylidic CH_2^-.

As already observed in the coordination sphere of the sulfur and the nitrogen atoms, the charge density related bond angles represent the hybridization state. The lone pair related angles with the distinct CCs toward the hydrogen atoms are widened in accordance with the VSEPR theory (LP_{C5}−C5−$CC_{C5\to H101}$ = 114.3°, LP_{C5}−C5−$CC_{C5\to H102}$ = 114.6°), while LP_{C5}–C5–$CC_{C5\to S1}$, including the less pronounced CC toward S1 (−17.3 e/Å^5), is contracted to 101.9°. Those angles, which are made up of C5, $CC_{C5\to H101/102}$, and $CC_{C5\to S1}$, are 110.9° and 110.7°, very close to the tetrahedral angle, while the one between the two covalent C−H bonds is 104.6°. This is an exemplary case where the geometric impression alone could lead to a false interpretation. The two ylidic hydrogen atoms seem to be inclined away from the sulfur atom relative to the C_2Li_2 base. This impression is caused by the strongly distorted octahedral environment of the carbanion. Nevertheless, this cannot hold after inspection of the VSCC angles as presented above, because the environment of the carbanion is tetrahedral concerning the VSCCs, and thus all bonding partners are at their predicted positions.

The lone pair at the ylidic carbon atom interacts obviously with all three lithium atoms of the capped Li_3 triangle, since bond paths between each of them and C5 are formed. The Li−C bond paths are curved (cf. Figure 3), but the calculated path lengths are less than 1% longer than the core distances. At 2.42446 and 2.40134 Å, the Li1/2–C5 paths are about 0.14 and 0.12 Å longer than the Li4−C5 contact (2.28786 Å). This shortening of Li4−C5 gives rise to an increase of density at the BCP ($\rho(\mathbf{r}_{BCP})$ = 0.078 (Li1), 0.080 (Li2), 0.107 e/Å^3 (Li4)) as well as of the positive Laplacian, $\nabla^2\rho(\mathbf{r}_{BCP})$ (+1.663 (Li1), +1.747 (Li2), +2.299 e/Å^5 (Li4)), although on a low level. These values are in the range usually quoted for predominantly ionic interactions, which is not surprising if a Li^+ and CH_2^- interaction is under investigation.[21] An inspection of the ratio of the eigenvalues of the Laplacian at the BCPs shows that the density between C5 and Li4 is much more separated than between C5 and Li1 and C5 and Li2 (cf. Figure 8a,b), which can be deduced from an almost 2 times higher eigenvalue λ_3 for the short Li−C bond. This is even more striking, since the Li4−C5 path is much shorter, which at first sight should result in an increased density overlap.

The two different Li−C bonding characteristics (Li1−C5, Li2−C5: fuse face, Li4−C5: cube corner) are reflected by the Laplacian distributions along the bond paths (cf. Figure 8c). The minimum for Li4−C5 is more distinct than the other two minima and located closer to the BCP. Both observations are caused by the on average 0.12 Å shorter Li4−C5 bond. However, all three distributions reveal the same qualitative behavior. The Laplacian stays positive over the whole bonding region up to the valence shell of C5.

In contrast to Bickelhaupt's findings,[29] this can be taken as a strong hint for the closed-shell nature of the Li−C interaction.

On the other hand, no bond paths could be determined between the lithium atoms (cf. Figure 6). Therefore we state that the unique driving force for the formation of the Li_3−C tetrahedron is the Li−C closed-shell interactions.

Conclusion

In the present paper a study on the synthesis, polymorphism, and experimental charge density of $[(thf)Li_2\{H_2CS(N^tBu)_2\}]_2$ (**1**) was presented. This compound is chemically and structurally of striking interest because it resembles a sulfur ylide and shows the Li_3C_α motif, well known from organolithium chemistry.

Two additional polymorphous modifications (**1b**, **1c**) to the form known from literature of $[(thf)Li_2\{H_2CS(N^tBu)_2\}]_2$ (**1a**) were discovered. The polymorphs differ almost exclusively by the orientations of the coordinating thf molecules and their degree of disorder. The polymorphous transitions show the characteristics of displacement transitions (little atom rearrangement) and are of first order, which implies superheating/supercooling during the destructive transitions. In **1a** and **1b** a

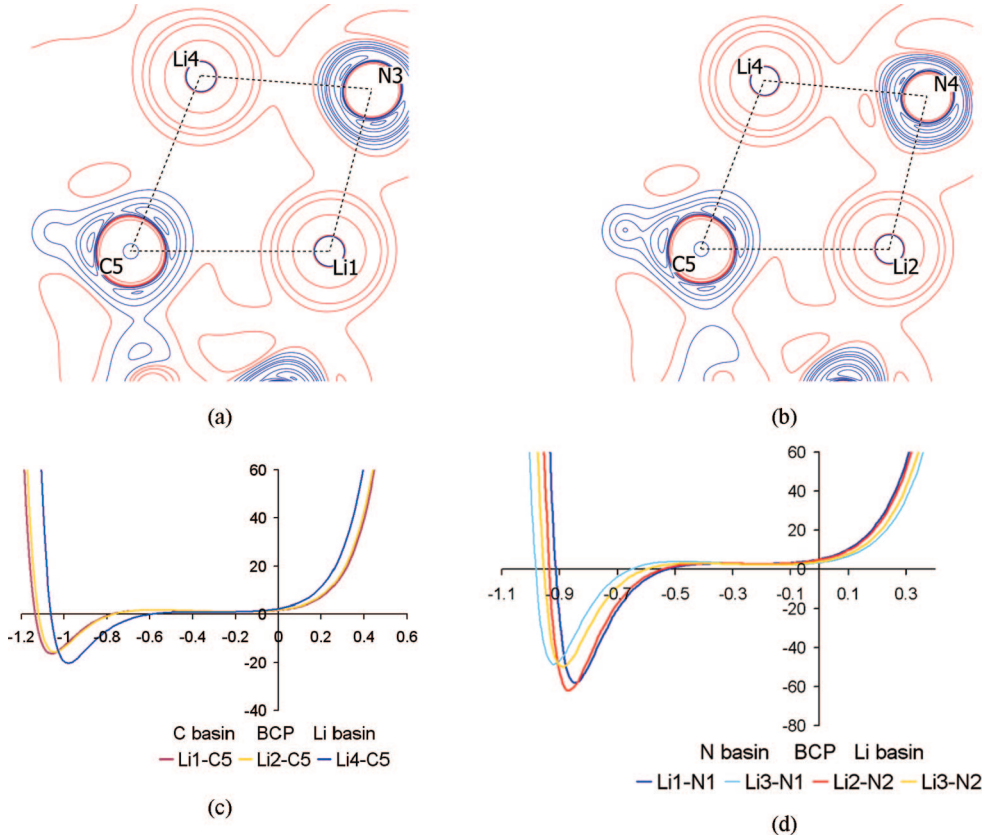

Figure 8. $\nabla^2\rho(\mathbf{r})$ distributions in the C5Li1Li4 (a) and C5Li2Li4 (b) planes and along the C−Li (c) and N−Li (d) bond paths. Contour plots (a) and (b): blue contours show negative values (electron density concentrations), red contours positive ones (electron density depletions); profile plot (c) and (d): $\nabla^2\rho(\mathbf{r})$ [e/Å^5] along the C−Li and N−Li bond paths (*x*-axis: distance from the BCP).

disorder of the thf molecules is present. No signs of twinning or disorder were present for the crystals of **1c**, and thus an experimental charge density study could be performed on high-resolution X-ray diffraction data.

By analyzing the topological properties of the experimental electron density distribution according to Bader's QTAIM, it was possible to specify the S−N and S−C bonds in **1** as classical single bonds strengthened by electrostatic interactions (S^+-N^- and S^+-C^-). This, together with the observation that four VSCCs are present at the sulfur atom, clearly rules out hypervalency, which is in good agreement with our previous findings for other formally hypervalent SN compounds. The present compound should be formulated as ylidic rather than ylenic. This describes the electronic situation best and explains the reactivity of the compound.

Furthermore, the interaction of the carbanion with the Li_3 triangle was determined to be of $CH_2^-\cdots(Li^+)_3$ type. The carbon atom forms a bond to each of the three lithium atoms, although one interaction is preferred. Thus, the VSCC at the carbanion that is representing the lone pair is inclined away from the center of the Li_3 triangle toward the lithium atom at the tip of the isosceles triangle. This is also reflected by the characteristics of the BCPs. No BCPs and thus no bonding interactions in the framework of QTAIM between the lithium atoms were determined. Therefore, the driving force for the formation of an Li_3 triangle seems to be the interaction of the lithium cations with the carbanion.

Synthesis

The applied experimental conditions and analytic methods are described in the Supporting Information.

Although $[(thf)Li_2\{H_2CS(N^tBu)_2\}]_2$ (**1**) may be obtained starting from $S(N^tBu)_2$ according to the method described in the literature,[7] we developed the following one-pot synthesis, which gives higher overall yields (82% compared to 66%): 2.2 equiv of MeLi (1.6 M in Et_2O) is added to a solution of $S(N^tBu)_2$ in THF at −78 °C over 15 min. A white precipitate forms in the initially clear solution and methane gas evolution can be observed. The reaction mixture is stirred another 15 min at −78 °C and for 16 h at room temperature. The solvent is then removed and the residue recrystallized from thf/hexane (yield: 82%). Colorless crystals of the polymorph **1a** can be obtained from a 2:5 mixture of thf and hexane at −5 °C after 2 days. If a 1:2 mixture of thf and hexane is stored at −16 °C for 7 days, colorless crystals of **1b** can extracted. The polymorphous modification **1c** accrues if crystallization is performed below 245 K from a very dilute 4:1 thf/hexane mixture.

Melting point: 114 °C (dec). ^{1}H NMR (300 MHz, C_6D_6): δ 0.94 (s, 4H; S−CH_2), 1.24 (t, 8 H; O−CH$_2$−CH_2), 1.42 (s, 36 H; C(CH_3)$_3$), 3.50 (t, 8 H; O−CH_2−CH$_2$). ^{13}C NMR (100 MHz, C_6D_6): δ 25.4 (O−CH$_2$−CH_2), 33.9 (C(CH_3)$_3$), 52.6 (*C*(CH3)3), 68.7 (O−CH_2−CH$_2$). ^{7}Li NMR (116.7 MHz, ext. sat. LiCl solution): δ 1.67, 2.73 (2 s, 4 *Li*). Anal. Calcd. for $C_{26}H_{56}Li_4N_4O_2S_2$ (548.63 g/mol) [%]: C 56.9, H 10.3, N 10.2, S 11.7. Found [%]: C 56.1, H 10.5, N 10.4, S 10.9. The DSC is discussed in the Supporting Information and ref 12. ^{6}Li-MAS NMR and ^{13}C-CP/MAS NMR can be found in ref 7.

The X-ray crystallographic data, bond lengths, angles, atom coordinates, thermal parameters, and multipole populations are given in an additional CIF file (charge density specific version for **1c**), which has been deposited with the Cambridge Crystallographic Data Centre (**1b**: CCDC 656363, **1c**: CCDC 656364) and can be accessed via www.ccdc.cam.ac.uk/data request/cif.

Acknowledgment. This work was supported by the Deutsche Forschungsgemeinschaft within the priority program 1178 Experimental charge density as the key to understand chemical interactions. All authors are grateful for the continuous support of the CHEMETALL GmbH at Frankfurt and Langelsheim, and INCOATEC GmbH at Geesthacht, Germany.

Supporting Information Available: Description of the multipole refinements, definition of the local coordinate systems, quality criteria after multipole refinement, Hirshfeld-test, residual densities, monopole populations (and contraction/expansion parameters), critical points not discussed in the paper, VSCC properties, and integration of the atomic basins. This material is available free of charge via the Internet at http://pubs.acs.org.

OM800046N